$$P_z(h) = \frac{(1-\alpha)^2}{1-\alpha^2/f}\frac{1-(\alpha^2/f)\exp(-b^2h^2/3)}{[1-\alpha\exp(-b^2h^2/6)]^2} \quad \text{(A2.12)}$$

where b is the effective bond length and $h = (4\pi/\lambda)\sin\theta/2$.

Mean Square Radius of Gyration. The mean square radius of gyration may be found from the power expansion of the particle scattering factor

$$P_z(h) = 1 - \tfrac{1}{3}\langle S^2\rangle_z h^2 + \ldots \quad \text{(A2.13)}$$

Expansion of eq A2.12 gives

$$P_z(h) = \left(1 + \frac{\alpha^2/f}{1-\alpha^2/f}b^2h^2/3\right) \Big/ \left(1 + \frac{\alpha}{1-\alpha}b^2h^2/6\right)^2 \quad \text{(A2.14)}$$

and

$$P_z(h) = 1 - \left(\frac{\alpha}{1-\alpha} - \frac{\alpha^2/f}{1-\alpha^2/f}\right)b^2h^2/3 + \ldots \quad \text{(A2.15)}$$

Hence

$$\langle S^2\rangle_z = b^2\left(\frac{\alpha}{1-\alpha} - \frac{\alpha^2/f}{1-\alpha^2/f}\right) \quad \text{(A2.16)}$$

Since $\alpha \simeq 1$ eq A2.14 can be written as

$$P_z(h) = (1 + \langle S^2\rangle h^2/6)^{-2} \quad \text{(A2.17)}$$

References and Notes

(1) See for instance: (a) M. Huglin, "Light Scattering from Polymer Solutions", Academic Press, London, 1972; (b) K. A. Stacey, "Light Scattering in Physical Chemistry", Butterworths, London, 1956.
(2) M. Kerker, "The Scattering of Light and other Electromagnetic Radiation", Academic Press, New York, N.Y., 1969.
(3) W. H. Stockmayer, *J. Chem. Phys.*, **11**, 45 (1943); **12**, 125 (1944).
(4) P. J. Flory, "The Principles of Polymer Chemistry", Cornell University Press, Ithaca, N.Y., 1953.
(5) H. Benoit, *J. Polym. Sci.*, **11**, 561 (1953).
(6) H. Dautzenberg and Ch. Ruscher, *Rheol. Acta*, **4**, 119 (1965); *J. Polym. Sci., Part C*, **16**, 2913 (1967); *Faserforsch. Textiltech.*, **16**, 1 (1965).
(7) (a) G. C. Berry and T. A. Orofino, *J. Chem. Phys.*, **40**, 1614 (1964); (b) E. F. Casassa and G. C. Berry, *J. Polym. Sci., Part A-2*, **4**, 881 (1966).
(8) K. Kajiwara, W. Burchard, and M. Gordon, *Br. Polym. J.*, **2**, 110 (1970).
(9) W. Burchard, *Macromolecules*, **5**, 604 (1972).
(10) W. Burchard, *Macromolecules*, **7**, 835, 841 (1974).
(11) K. Kajiwara and M. Gordon, *J. Chem. Phys.*, **59**, 3626 (1973).
(12) K. Kajiwara and C. M. A. Ribeiro, *Macromolecules*, **7**, 121 (1974).
(13) M. Gordon, K. Kajiwara, C. A. L. Peniche-Covas, and S. B. Ross-Murphy, *Makomol. Chem.*, **176**, 2413 (1975).
(14) W. Burchard, B. Ullisch, and Ch. Wolf, *Faraday Discuss. Chem. Soc.*, **No. 57**, 56 (1974).
(15) Ch. Wolf and W. Burchard, *Makromol. Chem.*, **177**, 2519 (1976).
(16) I. Franken and W. Burchard, *Br. Polym. J.*, in press.
(17) B. Ullisch and W. Burchard, *Makromol. Chem.*, **178**, 1403, 1427 (1977).
(18) K. Kajiwara, *Polymer*, **12**, 57 (1971).
(19) M. Gordon, K. Kajiwara, and A. Charlesby, *Eur. Polym. J.*, **11**, 385 (1975).
(20) W. Burchard, K. Kajiwara, M. Gordon, J. Kálal, and J. W. Kennedy, *Macromolecules*, **6**, 642 (1972).
(21) See for instance: P. J. Flory, "Statistical Mechanics of Chain Molecules", Interscience, New York, N.Y., 1969.
(22) M. Rinaudo and W. Burchard, manuscript in preparation.
(23) J. Heller and M. Schramm, *Biochim. Biophys. Acta*, **81**, 96 (1964).
(24) G. L. Brammer, M. A. Rougvie, and D. French, *Carbohydr. Res.*, **24**, 343 (1972).
(25) G. Porod, *Monatsh. Chem.*, **80**, 251 (1949).
(26) S. Heine, O. Kratky, G. Porod, and P. J. Schmitz, *Makromol. Chem.*, **46**, 682 (1961).
(27) W. Burchard and K. Kajiwara, *Proc. R. Soc. London, Ser. A*, **316**, 185 (1970).
(28) (a) H. Eschwey, M. L. Hallensleben, and W. Burchard, *Makromol. Chem.*, **173**, 235 (1973); (b) H. Eschwey and W. Burchard, *Polymer*, **16**, 180 (1975).
(29) H. Eschwey, Diploma Thesis, Freiburg, 1973.
(30) M. Müller, Diploma Thesis, Freiburg, 1976.
(31) G. C. Berry et al., *J. Polym. Sci.*, submitted for publication.
(32) J. Schelten, D. G. H. Ballard, G. D. Wignall, G. Longman, and W. Schmatz, submitted for publication.
(33) C. L. Pekeris, *Phys. Rev.*, **71**, 268 (1947).
(34) P. Debye and A. M. Bueche, *J. Appl. Phys.*, **20**, 518 (1949).
(35) See for instance: A. Guinier and G. Fournet, "Small Angle Scattering of X-rays", Wiley, New York, N.Y., 1955.
(36) P. Debye, *J. Phys. Chem.*, **51**, 18 (1947).
(37) B. H. Zimm, *J. Chem. Phys.*, **16**, 1093 (1948).
(38) M. Gordon, *Proc. R. Soc. London, Ser. A*, **268**, 240 (1962).
(39) G. R. Dobson and M. Gordon, *J. Chem. Phys.*, **41**, 2389 (1964).
(40) For a broken rod model, for instance, the length of the rodlike sections must be $\langle S^2\rangle_{rod}^{1/2} = L_{rod}/(12)^{1/2} < \lambda/20$, i.e., $L_{rod} > 57.2$ nm if the wavelength is λ 330 nm. Thus, a chain with four to five rodlike sections must have dimensions of $\langle S^2\rangle^{1/2} > 100$ nm before the rodlike sections will be detectable by light scattering.

Determination of Macromolecular Structure in Solution by Spatial Correlation of Scattering Fluctuations

Zvi Kam

Polymer Department, Weizmann Institute of Science, Rehovot, Israel.

Received April 11, 1977

ABSTRACT: I propose a new type of scattering technique which includes measurements of scattering intensities at two angles and accumulates the spatial correlation of fluctuations of elastic scattering from solutions. A theoretical analysis of the proposed method shows that it contains structural information much more detailed than the classical diffuse, orientationally averaged scattering intensity pattern. In principle it approaches the information obtainable from difffraction studies of single crystals. A data acquisition and reduction scheme is described. It solves the coefficients of expansion in spherical harmonics that give the oriented, single-particle scattering intensity pattern. The experimental conditions required to perform the proposed measurements and the resolution limitations are discussed. A simple example is presented as an illustration.

(I) Introduction

X-ray and thermal neutron scattering are among the most direct probes of the atomic structure of molecules. Still, in practice, their use for determination of the structure of macromolecules depends on one hand on the availability of single crystals, or on the other hand one has to suffice with low-angle diffuse scattering from solutions in which the detailed atomic information is obscured by orientational averaging of the scattering pattern, and lower resolution is achieved.

Recent development in scattering experiments incorporating intense x-ray and neutron sources and rapid positional-sensitive detectors makes it possible to record the

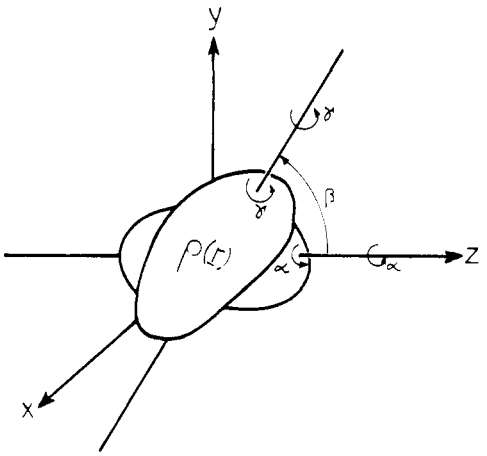

Figure 1. Transformation of rigid particle to an arbitrary orientation using the three successive Eulerian rotations, with angles α, β, and γ. α is a rotation around the z axis, β is rotation around the y axis, and γ is rotation around the new z axis.

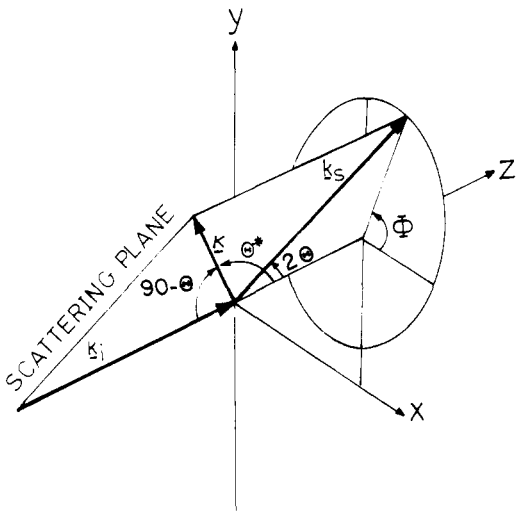

Figure 2. Illustration of the scattering configuration. The z axis was taken along the incident beam vector, k_i. The polar angles $(2\theta,\Phi)$ of the scattered beam vector k_s and (θ^*,Φ) of the scattering vector $\kappa = k_s - k_i$ are marked.

scattering pattern from solutions over a wide range of scattering angles, in times comparable to macromolecular reorientation. In this note I investigate the theoretical possibility of performing measurements that reveal information about the scattering pattern of macromolecules in solution which is much more detailed than that hitherto obtainable from classical low-angle scattering experiments. Probing the structural details that are usually averaged in conventional scattering measurements becomes possible by considering the fluctuations in the distribution of orientation of individual scatterers, which cause the momentary scattering intensity to fluctuate about the average. The enhancement of the signal from fluctuations derived from random rotation of the particle can be performed experimentally by time averaging the product of the instantaneous intensity pattern at two scattering directions. This data acquisition technique which may be called "spatial correlation" can be used to derive the oriented single-particle scattering pattern. The technique is applicable to x ray, neutron, and light scattering from macromolecules. We may expect different resolution with complementary information from the three experimental methods. The experiments become easier to perform, the larger the scatterers are. Thus the technique complements crystallography, which under such circumstances is becoming harder to apply.

We first formally develop the relations between the proposed measurable correlations and the single-particle scattering function. The results are then explored qualitatively, and a specific example is demonstrated.

(II) Formal Derivation

Consider a suspension (solution) of N identical particles, each having an electron density function $\rho(r)$, randomly oriented in space. The scattering intensity pattern from one of these particles as a function of the scattering vector κ is given by:

$$S(\omega,\kappa) = |\int d\mathbf{r}\rho(\mathbf{R}(\omega)r)e^{i\kappa\cdot r}|^2 \equiv |A(\omega,\kappa)|^2 \qquad (1)$$

where $\mathbf{R}(\omega)$ is the rotation operator which rotates the particle from the arbitrarily defined initial position $\rho(r)$ to any other orientation. In the treatment below it will be most convenient to use the three Eulerian angles of rotation of a rigid body $\omega = (\alpha\beta\gamma)$ (Figure 1). The scattering vector κ, given by the difference of the scattered and incident vectors k_s and k_i, is

$$\kappa = k_s - k_i \qquad (2)$$

and its magnitude is:

$$|\kappa| = 2|k_i| \sin\theta = 2|k_i||\cos\theta^*| = 2|k_s| \sin\theta \qquad (3)$$

The scattered photon direction k_s is defined by the angles $\Omega = (2\theta, \Phi)$, and the direction of κ by Ω^* (Figure 2):

$$\Omega^* = (\theta^*, \Phi) = (90 + \theta, \phi) \qquad (4)$$

The classical diffuse time-average scattering from this solution is obtained from $S(\omega,\kappa)$ by averaging over the particle orientations and is axially symmetric around the z axis:

$$S(\kappa) = \frac{N}{8\pi^2}\int S(\omega,\kappa)\, d\omega \equiv S(|\kappa|) \qquad (5)$$

where

$$\int d\omega \equiv \int_{-\pi}^{\pi} d\gamma \int_0^{\pi} \sin\beta\, d\beta \int_0^{2\pi} d\alpha = 8\pi^2 \qquad (6)$$

In the above expression the distribution of the orientation of the particles averaged over time was taken as isotropic. On the other hand, at each given moment the actual orientation distribution of the particles fluctuates around the average isotropic one, so that the number of particles in a defined orientation increment $d\omega$ around ω can be written as

$$N_t(\omega)\, d\omega = \left[\frac{N}{8\pi^2} + \alpha_t(\omega)\right] d\omega \qquad (7)$$

and the momentary scattering pattern will be (neglecting interparticle coherent scattering fluctuations[1]):

$$S_t(\kappa) = S(|\kappa|) + \int S(\omega,\kappa)\alpha_t(\omega)\, d\omega \qquad (8)$$

The second term in the right hand side of eq 8 is the fluctuating part of the scattering pattern. Each time a fluctuation in the number of molecules in a certain orientation ω occurs, a corresponding change will be detected in $S_t(\kappa)$ such that for *different* values of κ this change will be proportional to $S(\omega,\kappa)$. Suppose $S(\omega,\kappa)$ has peaks for a certain ω_0 at values k_0 and k_0' and let us assume for the sake of the argument that there is no other value of ω for which $S(\omega,\kappa)$ has such peaks at both k_0 and k_0' (although a peak may occur for one of these values). By looking at $S_t(\kappa)$ we detect from time to time peaks for k_0 and k_0', which then broaden and decay in time depending on the rotational diffusion coefficient (see next section). That part of the fluctuations for different values of κ which corresponds to the same ω can be extracted (out of the fluctuations due to different ω) by cross correlating and time-averaging the products of the momentary scattering intensities. This will

enhance the variations of $S(\omega,\kappa)$ for two different values of κ that rise and fall together due to rotations of the same particle and average out random changes due to fluctuations in angular distribution of different particles.

Let us define

$$D(\kappa_1,\kappa_2) = \langle S_t(\kappa_1)S_t(\kappa_2)\rangle \tag{9}$$

where the brackets $\langle\ \rangle$ denote the time average. Substituting eq 8, and using the fact that the time average of $\alpha_t(\omega)$ is zero, that there is no correlation between the fluctuations in the number of particles in two different orientations, and that the mean-square fluctuations are proportional to the number of particles, i.e.,

$$\langle \alpha_t(\omega_1)\alpha_t(\omega_2)\rangle = \frac{N}{8\pi^2}\delta(\omega_1 - \omega_2) \tag{10}$$

we get

$$D(\kappa_1,\kappa_2) = S(|\kappa_1|)S(|\kappa_2|) + C(\kappa_1,\kappa_2) \tag{11}$$

where:

$$C(\kappa_1,\kappa_2) = \frac{N}{8\pi^2}\int S(\omega,\kappa_1)S(\omega,\kappa_2)\,d\omega \tag{12}$$

As $S(|\kappa|)$ and $C(\kappa_1,\kappa_2)$ are measurable quantities, we see that one can extract from such experiment not only the angular average of the scattering pattern (eq 5) but also the average of its products for two arbitrary scattering directions.

We use the common expansion in spherical harmonics[2,3] to give eq 12 a practically useful form. Let us write

$$S(0,\kappa) = \sum_{lm} S_{lm}(|\kappa|)Y_{lm}(\Omega^*) \tag{13}$$

Then, upon rotation of the particle the spherical harmonics transform according to the rotation matrices[4] $R^l_{m'm}(\omega)$

$$S(\omega,\kappa) = \sum_{lmm'} S_{lm}(|\kappa|)Y_{lm'}(\Omega^*)R^l_{m'm}(\omega) \tag{14}$$

We use the orthogonality of $R^l_{m'm}(\omega)$[4]

$$\int R^l_{m'm}(\omega)R^l_{M'M}{}^*(\omega)\,d\omega = \delta_{l'l}\delta_{mM}\delta_{m'M'}x\,\frac{8\pi^2}{2l+1} \tag{15}$$

and the addition theorem[4]

$$\sum_{m'} Y_{lm'}(\Omega_1{}^*)Y_{lm'}{}^*(\Omega_2{}^*) = \frac{2l+1}{4\pi}P_l(\cos\psi) \tag{16}$$

where ψ is the angle between the directions $\Omega_1{}^*$ and $\Omega_2{}^*$ of κ_1 and κ_2, respectively. Substituting eq 14 into eq 12 using eq 15 and 16 we obtain:

$$C(\kappa_1,\kappa_2) = \frac{N}{4\pi}\sum_l P_l(\cos\psi)\left[\sum_{m=-l}^{l} S_{lm}(|\kappa_1|)S_{lm}{}^*(|\kappa_2|)\right] \equiv C(|\kappa_1|,|\kappa_2|,\psi) \tag{17}$$

This result may be written together with the corresponding formula for diffuse scattering

$$S(|\kappa|) = (4\pi)^{1/2}S_{00}(|\kappa|) \tag{18}$$

in order to compare the information contained in $C(\kappa_1,\kappa_2)$ to that of the average diffuse scattering, $S(|\kappa|)$. $S(|\kappa|)$ contains only the orientationally averaged isotropic scattering component, whereas eq 17 exhibits the contribution of all the spherical harmonic components of the *oriented* single particle. Moreover, the contribution of each angular momentum, l, has a well-defined angular dependence given by the lth Legendre polynomial. As we discuss in the next section, this property enables one to eliminate *directly* (although not quite uniquely) all the $S_{lm}(|\kappa|)$ components. This is far more powerful than the usual iterative procedure that best fits the experimental $S(|\kappa|)$ to model calculations of different scatterer shapes.

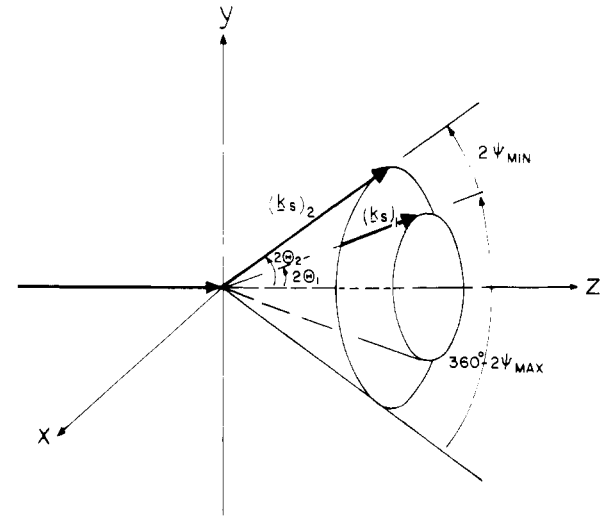

Figure 3. The range of angles ψ between two scattering vectors of given magnitude. The scattered beams span two cones forming angles $2\theta_1$ and $2\theta_2$ with the incident beam direction.

(III) Treatment of Experimental Data

Equation 17 can be used experimentally on two levels of data reduction with: (A) a total intensity scattering experiment with monochromatic incident radiation, and (B) an experiment in which the incident spectrum is "white" and the wavelength separation just precedes the detection. The second arrangement is more complex instrumentally, but it provides measurements that allow for more powerful data reduction.

In a classical configuration for scattering of a monochromatic beam, the magnitude of the scattering vector $|\kappa|$ depends on the angle of scattering 2θ according to eq 3 but is independent of Φ, the angle of rotation around the incident beam axis. A measurement of the cross correlation $C(\kappa_1,\kappa_2)$ can be made for given values of $|\kappa_1|$ and $|\kappa_2|$ for a range of angles ψ between κ_1 and κ_2 that lie on two cones of scattering at fixed angles $\theta_1{}^*$ and $\theta_2{}^*$. As is illustrated in Figure 3, the maximum range of ψ spanned between two such cones depends on the values $|\kappa_1|$ and $|\kappa_2|$ but is always smaller than the full range of $0° < \psi < 180°$. The measured data can be used in the same way diffused average scattering is used today to give a plausibility figure to theoretical predictions and model calculations. The measurement of $C(\kappa_1,\kappa_2)$ is expected to supply much more critical criteria for the plausibility of different models.

If, on the other hand, one allows a continuous wavelength spectrum to be scattered, any desired scattering vector $|\kappa|$ at any desired angle of scattering 2θ can be measured when the detectors are preceded by monochromators allowing to pass such wavelength for which k_s satisfies eq 3 for given $|\kappa|$ and θ. In such a configuration one can measure $C(\kappa_1,\kappa_2)$ for arbitrary values of $|\kappa_1\|\kappa_2|$ and the angle between them, ψ. As $0° < 2\theta < 180°$ and $90° < \theta^* < 180°$, values for $0° < \theta^* < 90°$ can be obtained from the relation

$$S(\omega,\kappa) = S(\omega,-\kappa) \tag{19}$$

so that $C(\kappa_1,\kappa_2)$ can be obtained for $0° < \psi < 180°$. Keeping $|\kappa_1|$ and $|\kappa_2|$ unchanged, eq 17 can be used to separate explicitly the different components of the scattering intensity angular momentum. Using the orthogonality relations for Legendre polynomials[4]

$$\int_{-1}^{1} P_l(u)P_{l'}(u)\,du = \frac{2}{2l+1}\delta_{ll'} \tag{20}$$

we get (using eq 19) vanishing contribution of odd l values, and for even values of l:

Table I[a]

	Structure	Amplitudes	Intensities	Measurements
Crystallography	$\rho(r)$	$A(\kappa)$	$S(\kappa)$	$S(\kappa_i)$
Scattering from solutions	$\rho(r)$	$A(\kappa)$	$S(\kappa)$	$S_{00}(\lvert\kappa\rvert)$, $C(\kappa_1,\kappa_2)$

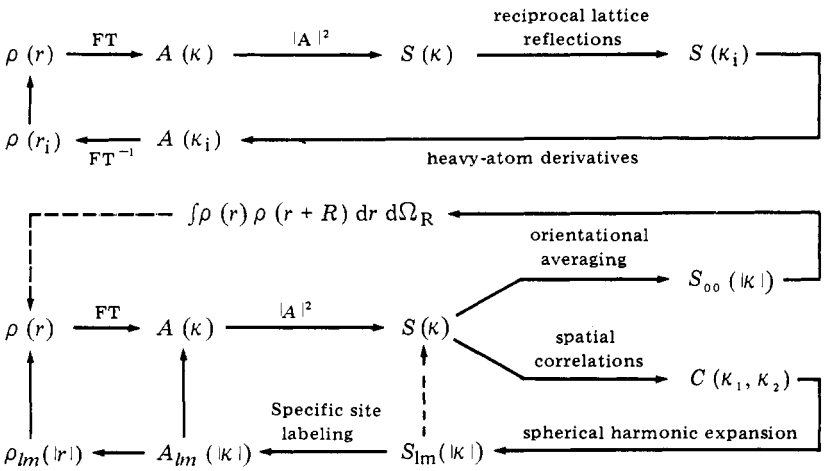

[a] FT = Fourier transform; $X \rightarrow Y$, unique determination of Y from X; $X \dashrightarrow Y$ = ambiquous or partial determination of Y from X. The symbols have the same meaning as in the text.

$$C_l(|\kappa_1|,|\kappa_2|) \equiv 2\pi \frac{(2l+1)}{N} \int_0^\pi C(\kappa_1,\kappa_2) P_l(\cos\psi) \sin\psi \, d\psi$$

$$= \sum_{m=-l}^{l} S_{lm}(|\kappa_1|) S_{lm}^*(|\kappa_2|) \qquad l = 0, 2, 4, \ldots \quad (21)$$

The explicit solution of $S_{lm}(|\kappa|)$ for a certain l is now described: Let us envisage $S_{lm}(|\kappa_i|)$ as vectors of $(2l + 1)$ components ($m = -l, \ldots, l$) and let us measure $C(\kappa_1,\kappa_2)$ and calculate $C_l(|\kappa_1|,|\kappa_2|)$ for all possible pairs from a set of values, κ_i. The sums

$$\sum_m S_{lm}(|\kappa_i|) S_{lm}^*(|\kappa_j|) = C_l(|\kappa_i|,|\kappa_j|) \quad (22)$$

give for $i = j$ the magnitudes of the vectors. For $i \neq j$ the scalar products give the cosine of angles between two such vectors. If we find one solution to the set of eq 22, then the set rotated with arbitrary angle ω_l

$$S_{lm'}(|\kappa_i|) = S_{lm'}(|\kappa_i|) R^l_{m'm}(\omega_l) \quad (23)$$

is also a valid solution, since

$$\sum_m R^l_{mm'}(\omega) R^{l}_{mm''}{}^*(\omega) = \delta_{m'm''} \quad (24)$$

The physical meaning of eq 23 is that the solution is unique up to an arbitary rigid rotation; as for a suspension of unoriented particles the reference frame of coordinates is of no significance. This is not the case in the crystal diffraction pattern, where the frame of coordinates rotates together with the crystal. We can prescribe a special solution to eq 22 by forming $(2l + 1)$ independent vectors for $(2l + 1)$ values of κ_i. The first vector is:[7]

$$S_{l(-l)'}(|\kappa_1|) = \pm(C_l(|\kappa_1|,|\kappa_1|))^{1/2} \quad (25)$$

The other components vanish. The second vector has two components:

$$S_{l(-l)'}(|\kappa_2|) = C_l(|\kappa_2|,|\kappa_1|)/S_{l(-l)}(|\kappa_1|) \quad (26)$$

$$S_{l(-l+1)'}(|\kappa_2|) = \pm(C_l(|\kappa_2|,|\kappa_2|) - [S_{l(-l)}(|\kappa_2|)]^2)^{1/2} \quad (27)$$

The third has three components and so on. All together we have $(2l + 1)(l + 1)$ equations and the same number of unknowns. This solution is *unique up to signs* and can generate (via eq 23) the general solution. In addition to the sign ambiguities which originate from the fact that the correlation $C(\kappa_1,\kappa_2)$ is quadratic in scattering intensities, the random orientation of the molecules in the solution makes the experimental information invariant to free *relative* rotation of the different angular symmetry components with respect to each other (i.e., a different angle ω_l for each set of S_{lm}, $m = -l, \ldots, l$). Thus, if we approximate the scattering intensities with a sum of spherical harmonics trunquated after the first $2L$ terms (i.e., $l = 0, 2, 4, \ldots, 2L$) (see eq 13) the spatial correlation $C(\kappa_1,\kappa_2)$ yields a solution unique up to $(L + 1)(2L + 1)$ arbitrary signs and L arbitrary rotations. Actually the requirement for positive scattering intensities of the molecular scattering function $S(\omega,\kappa)$ for all ω and κ can be used to eliminate some of the degrees of freedom of the general solution. Also some rotations can transform one solution to another with inverted signs, and rotations of the $L = 0$ and 2 terms can be discarded without loss of generality, so that the number of independent solutions physically possible is greately reduced.

The uniqueness of the solution can be achieved if "specific site labeling" can be applied in a way analogous to the use of "Heavy Atom Derivatives" in x-ray crystallography. As we deal with large scattering masses, the meaning of specific site labeling may be addition of scattering centers in specific locations such as Ferritin antibodies or deutrated regions, so that the overall scattering pattern will have a sizable change. This technique, which is used for resolving the problem of phases of the scattering amplitudes A, calculated from the measured intensities of diffractions from crystals, can be used here also to determine signs and orientations of the different components of the single-particle scattering intensities S when calculated from the correlations C. In Table I we summarize the measurements and data reduction for x-ray crystallography, diffuse scattering from solutions, and spatial correlation measurements. In Appendix A the elimination of the scattering amplitudes is outlined using the specific site labeling derivative data.

This completes the constructive proof of the ability to solve the structure of particles in solution using the proposed scattering technique.

(IV) Experimental Feasibility and Signal-to-Noise Evaluation

The fluctuating part of $C(\kappa_1,\kappa_2)$ has to be measured within a time period comparable to the rotational diffusion of the scattering particles. If averaged over longer times the amplitude of the cross correlation of the fluctuations becomes

$$\mathrm{SNR} = \frac{\int_{\Delta\Omega_1} d\kappa_1 \int_{\Delta\Omega_2} d\kappa_2 \int_{\Delta\tau} dt \int S(\omega,\kappa_1)S(\omega,\kappa_2)\, d\omega \cdot \frac{N}{8\pi^2}}{\left(\int_{\Delta\Omega_1} d\kappa_1 \int_{\Delta\Omega_1} d\kappa_2 \int_{\Delta\tau} dt \int S(\omega,\kappa_1)\, d\omega \cdot \int S(\omega,\kappa_2)\, d\omega\right)^{1/2} \frac{N}{8\pi^2}} \tag{28}$$

vanishingly small. The amount of rotation needed to change the scattering pattern considerably depends on the required resolution and the scattering angle. Forward scattering intensity depends only on the total electron density of the scattering particle and not at all on its orientation. At higher scattering angles finer details of the structure are expressed and the scattering pattern is varying faster with angle. Also the total scattering intensity goes down rather sharply for increasing scattering angles although the *relative* amplitude of the fluctuations goes up. Hence, in order to obtain the finer structural details, one has to sample the fluctuating instantaneous scattering pattern during even shorter intervals at progressively wider scattering angles and with higher angular resolution. The decrease of intensity (encountered by satisfying the above requirements) sets the practical limit to the resolution one can expect in a given experiment.

The signal-to-noise ratio (SNR) for these experiments can be evaluated as follows: The signal is the fluctuation in the number of scattered x-ray photons (or neutrons). The noise is the statistical uncertainty which is mainly contributed by the average diffuse scattering. Neglecting the solvent and other parasitary background scattering we can write eq 28. The function $S(\omega,\kappa)$ is written in units of number of scattering events per particle per unit time per unit solid angle, $\Delta\tau$ is the duration of accumulation of the momentary scattering $S_t(\kappa)$, and $\Delta\Omega_1$ and $\Delta\Omega_2$ are the angular resolution of detection. We can define a coherence region $\Delta\Omega_c$ as the region over which $S(\omega,\kappa)$ stays constant:

$$\Delta\Omega_c \simeq \Delta\theta_c \Delta\Phi_c \tag{29}$$

As we discussed in the previous section, a change in θ introduces a change in $|\kappa|$. $\Delta\theta_c$ can be estimated as the change in κ for which the phase difference across the scatterers dimension, a, approaches unity. If the wavelength approaches the size of the particle, a more stringent limitation might be the condition that the required resolution d is achieved. Thus:

$$\Delta\theta_c \lesssim \frac{1}{2a|k_i| \cos\theta} \text{ or } \Delta\theta_c \lesssim \pi(d/a) \tag{30}$$

Rotation around the axis of the incident beam does not change $|\kappa|$, and variations in the scattering pattern depend on resolution only. If we aim at a resolution, d, then we have:

$$\Delta\Phi_c \lesssim \pi(d/a) \tag{31}$$

We can approach the evaluation of $\Delta\theta_c$ and $\Delta\Phi_c$ in a different way that ties directly with the spherical harmonics expansion of $S(\omega,\kappa)$. If we look at one term in the sum of eq 13, the function $Y_{lm}(\Omega^*)$ has at most L nodes as a function of θ^* or Φ, thus:

$$\Delta\theta_c \simeq \Delta\Phi_c \simeq \pi/L \tag{32}$$

If $\Delta\Omega_1$ is increased beyond $\Delta\Omega_c$ the integral $\int S(|\kappa_1|)\, d\kappa_1$ increases proportionally, but the integral $\int C(\kappa_1,\kappa_2)\, d\kappa_1$ is not quite proportional to $\Delta\Omega_1$ since the high resolution information in C in the form of fast variations is changing randomly and thus averages in Ω space. Similarly, by averaging longer than some characteristic time $\Delta\tau_R$, the fluctuations average out. $\Delta\tau_R$ can be estimated as follows: If the particle rotates in angle $\Delta\omega$ such that its maximum distance of motion is $\Delta r \simeq \Delta\omega a \simeq |\kappa|^{-1}$ the scattering pattern can change considerably. For diffusive motion $\Delta\omega \simeq (D_R\Delta\tau_R)^{1/2}$, D_R being the rotational diffusion coefficient. Substituting $\Delta\omega \simeq 1/|\kappa|a$ we obtain:

$$\Delta\tau_R \simeq \frac{1}{(2a|k_i| \sin\theta)^2 D_R} \text{ or } \Delta\tau_R \simeq \frac{(\pi d/a)^2}{D_R} \text{ or } \left(\frac{\pi}{L}\right)^2 \frac{1}{D_R} \tag{33}$$

As the available strongest x-ray and neutron sources, i.e., synchrotron Bremsstrahlung and high-flux nuclear reactors, emit a continuous spectrum of wavelengths, it is important to evaluate the maximum allowable wavelength range. The condition for coherent scattering from a particle of dimension a with required resolution d is:

$$\frac{\Delta\lambda}{\lambda} \lesssim \frac{d}{a} \text{ or } \frac{\Delta\lambda}{\lambda} \lesssim \frac{1}{L} \tag{34}$$

As both the numerator and the denominator in eq 28 are proportional to N, the number of scattering particles, the SNR is independent on N (as long as the background scattering is not dominant).

The optimal SNR is thus achieved when the scattered photons (or neutrons) are accumulated in regions $\Delta\Omega_c$ during time intervals $\Delta\tau_R$. In this case:

$$\mathrm{SNR} = \frac{\int S(\omega,\kappa_1)S(\omega,\kappa_2)\, d\omega}{[\int S(\omega,\kappa_1)\, d\omega \int S(\omega,\kappa_2)\, d\omega]^{1/2}} \Delta\tau_R(\Delta\Omega_1\Delta\Omega_2)^{1/2} \tag{35}$$

where depending on the conditions we get

$$\Delta\tau_R(\Delta\Omega_1\Delta\Omega_2)^{1/2} \simeq \frac{\pi d/a}{(2a|k_i|)^3 \cos\theta \sin^2\theta D_R}$$

or

$$\simeq (\pi d/a)^4/D_R \tag{36}$$

or

$$\simeq (\pi/L)^4/D_R$$

As $S(\omega,\kappa)$ is proportional to the incident beam flux, J, we see that the SNR ratio is proportional to J. This is of course the largest disadvantage of any fluctuation analysis method. Compared to diffraction from crystals, where the intensity of the diffraction spot is proportional to the square of the number of molecules (neglecting mosaic effects and assuming a coherent beam) and to the incident flux, in the fluctuation experiment, the spatial correlation (which is quadratic in measured intensities) is just proportional to the number of particles. Because of the value of the average background, the actual signal-to-noise ratio is only proportional linearly to the incident flux and is not proportional at all to the number of molecules. In practice it is necessary to scatter from many molecules because it is desirable that the scattering from the solvent and other sources of noise which were not taken in account in eq 35 should be made as small as possible.

Experimentally, we see that the incident wavelength has to be matched to the required resolution for the constraint of the rotation in the θ direction not to introduce the $1/(a|k_i| \cos\theta)$ factor into the SNR. We should also mention that the incident flux can be pulsed. This might be necessary due to sample heating by the incoming high flux.

If we want to evaluate the SNR for an experiment in which the resolution required is about 1/4 of the particles size (or equivalently, we match with spherical harmonics up to L = 4), we see that SNR $\simeq$ 1 if we can detect a few scattering

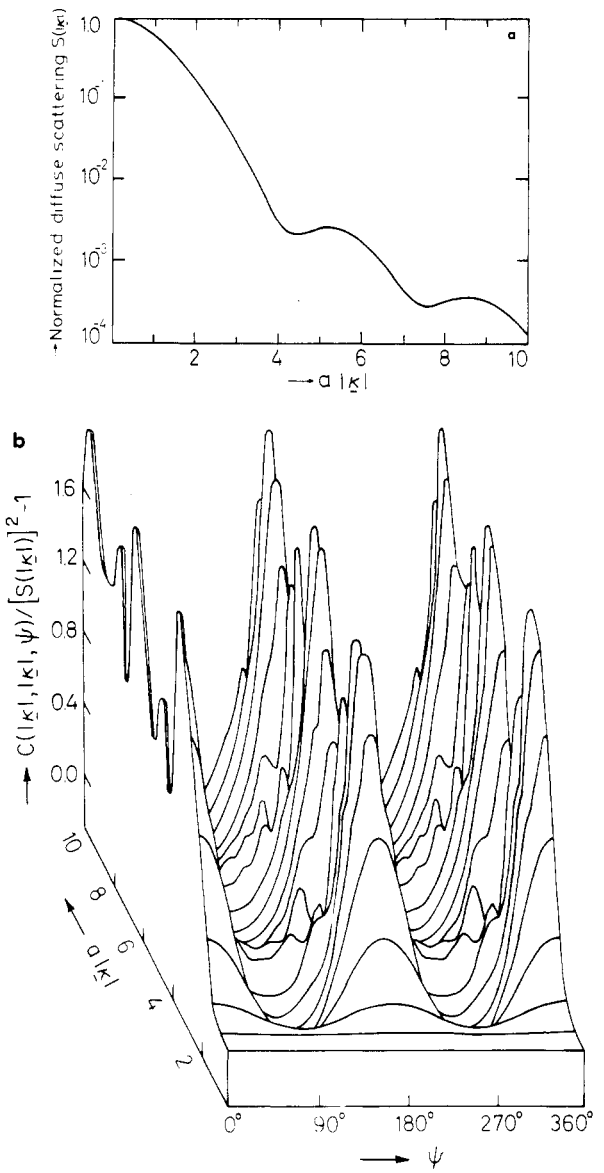

Figure 4. (a) The diffuse scattering pattern, $S(|\kappa|)$, as a function of the scattering vector magnitude, for an ellipsoid of revolution with semiaxes $(a, a, 2.5a)$. (b) The spatial correlation $C(\kappa_1,\kappa_2) = C(|\kappa_1|,|\kappa_2|,\psi)$ as a function of the angle ψ between two scattering vectors, of equal magnitude $|\kappa|$, for the above ellipsoid. The function C was plotted after the subtraction of the isotropic part ($l = 0$ term in eq 17 which is proportional to the square of the average intensity, eq 18) and normalization to the square of the average intensity. The twofold symmetry as well as higher order Legendre polynomial components are evident.

events in $1/D_R$ s, from each particle. A total of 10^{11} scattering events per second from about 10^9 molecules, and $D_R \simeq 10^2\ s^{-1}$, gives SNR $\simeq$ 1, which makes such an experiment feasible. A concentration of 0.17 mg/mL of a 10^6 molecular weight particle (0.17 μM concentration) in a 0.1 × 0.1 × 1.0 mm scattering volume contains 10^9 molecules and the scattering from the solution is about twice that of the solvent. 10^{11} scattering events require incident flux of 10^{16} photons (or neutrons) per second in the initial beam, in a wavelength range according to eq 34.

(V) An Illustrative Example

In order to anticipate the kind of data which will be obtained experimentally I have chosen a simple shape for a computer calculation: an ellipsoid of revolution.

The calculation of the scattering intensities was carried out according to Guinier.[5] Rewriting his result in our terminology we have:

$$S(\omega,\kappa) = \left[\frac{3(\sin u - u\cos u)}{u^3}\right]^2 \equiv \Theta(u) \tag{37}$$

where

$$u = |\kappa|a(1 + (\upsilon^2 - 1)\cos^2\delta)^{1/2} \tag{38}$$

the ellipsoids three semiaxes are $(a,a,\upsilon a)$ and δ is the angle that the vector κ forms with the axis of revolution of the ellipsoid. In terms of the scattering angle, 2θ, and the angles (β, ϕ) of the axis of revolution of the ellipsoid (assuming without loss of generality that κ lies in the y–z plane) we obtain

$$\cos\delta = \cos\theta\sin\beta\cos\phi - \sin\theta\cos\beta \tag{39}$$

Taking $\theta^* = 90°$ for κ_1 and $(90 + \psi)$ for κ_2 we can now write the expressions for $S(|\kappa|)$:

$$S(|\kappa|) = \int_0^1 \Theta\,(|\kappa|a(1 + (\upsilon^2 - 1)w^2)^{1/2}\,dw \tag{40}$$

and for $C(\kappa_1,\kappa_2)$:

$$C(|\kappa_1|,|\kappa_2|,\psi) = \frac{1}{4\pi}\int_{-\pi}^{\pi} d\phi \int_{-1}^{1} dw \cdot \Theta\,[|\kappa_1|a(1 + (\upsilon^2 - 1)(1 - w^2)\cos^2\phi)^{1/2}] \cdot \Theta[|\kappa_2|a(1 + (\upsilon^2 - 1) \cdot ((1 - w^2)^{1/2}\cos\psi\cos\phi - w\sin\psi)^2)^{1/2}] \tag{41}$$

w was substituted for $\cos\beta$. The values of $S(|\kappa|)$ were tabulated by Mittelbach and Porod.[6] In Figure 4, $S(|\kappa|)$ and $C(|\kappa|,|\kappa|,\psi)$ are plotted for an ellipsoid with axial ratio $\upsilon = 2.5$. Figure 4b demonstrates the behavior of the relative fluctuations as a function of the scattering vector. There are no fluctuations for $\kappa = 0$, and the relative fluctuations increase as κ becomes larger. The scattering intensity decreases with $|\kappa|$. Figure 4b demonstrates also the meaning of the coherence angle $\Delta\Omega$ which defines the allowable detector area as a function of the resolution required. In this simple case of an ellipsoid the obvious twofold symmetry is exhibited in $C(|\kappa|,|\kappa|,\psi)$ as a function of ψ. We recall that this information is totally obscured in $S(|\kappa|)$.

Finally, a visualization of the experimental data is given in Figure 5, using a simplified two-dimensional simulation which still demonstrates the features of the momentary scattering pattern.

A suspension of elliptical particles is represented by rice grains randomly spread on the table (right column of photographs in Figure 5). The scattering patterns (left column) were obtained by optical Fourier transform of a reduced transparency of the grains. The single grain transform is given in Figure 5a. The transform of the rectangular mask produces the line of reflections on the two perpendicular axes. The optical Fourier transform of two rice grains is given in Figure 5b and it is the sum of two rotated patterns of Figure 5a. The interparticle interference produces the striations which are finer the more distant the grains are. Figure 5c is the three grains transform and Figure 5d is the transform of six grains. The transforms approach very fast the axially symmetric pattern, yet even in Figure 5e, the transform of some 60 grains, the fluctuations in the pattern are apparent, and processing of these fluctuations produces the single grain scattering pattern.

The possibility of analyzing randomly oriented noisy patterns using the spatial correlation technique is directly applicable to electron micrographs image enhancement. The practical aspects of this process are the subject of a separate note.[8]

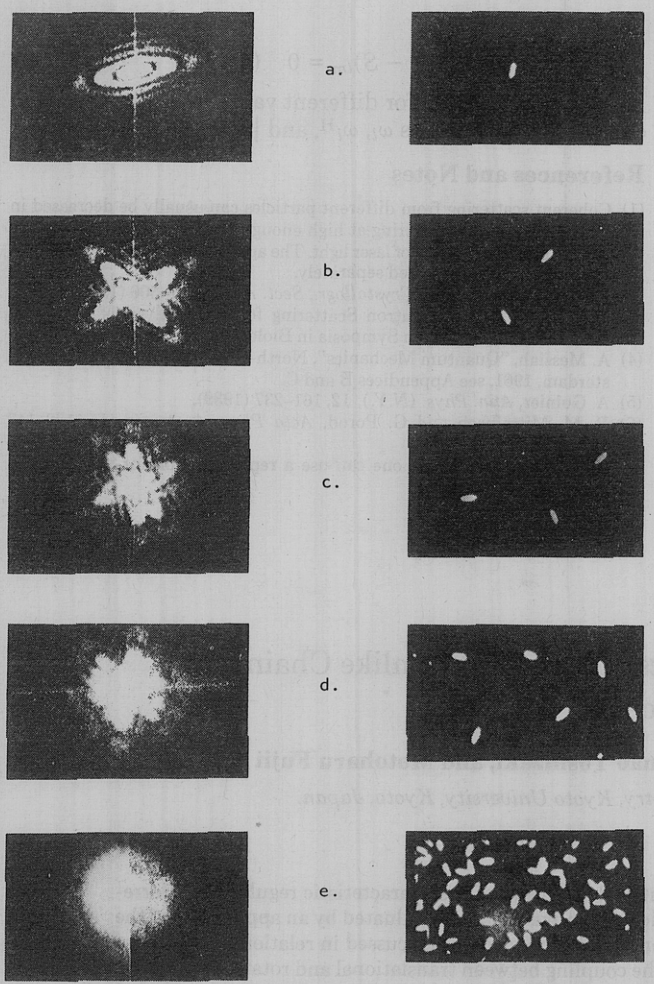

Figure 5. Optical Fourier transformation of randomly oriented rice grains. As the number of grains increases the pattern of the transform approaches the usual orientational average picture. Still the fluctuations in intensity are apparent even in the last transform. In order to cover a wider range of scattering intensities, the last transform, *e*, contains two half-frames of different exposure times. The radial variations in intensity can be directly compared with Figure 4a. The products of intensities at angles ϕ and $\phi + \psi$ averaged over ϕ gives the two-dimensional analogue of Figure 4b.

VI. Summary

In this paper I have proposed a new way of measuring and analyzing scattering from solutions of large molecules. The mathematics necessary to elucidate the information available from the proposed measurements are developed along with analysis of the experimental conditions needed to perform a feasible experiment.

Although in principle the technique is very promising, at this stage data acquisition that would allow structure determination at the resolution obtainable from x-ray crystallography of macromolecules does not seem possible. The method does permit though structural analysis at moderate resolution *in solution* and does not require organization of the macromolecules into a crystalline lattice. Thus the method is particularly advantageous for structural determination of assemblies consisting of many macromolecules like viruses, ribosomes, and muscle filaments where data at the 10 Å level would be useful. All the methods so well developed previously for x-ray diffraction and scattering studies, like specific site labeling, contrast variation, and isotope replacements, are directly applicable to this technique. One can expect to find spatial correlation measurements of great value for localization of nucleic acids and proteins in their complexes (like ribosomes, viruses, and chromatin), for obtaining structural information about membrane proteins in situ, and for studying structure of macromolecules by scattering from suspensions of microcystallines in cases where large enough crystals for diffraction work are not available.

We hope that the technical difficulties in this method may well be found less inhibiting than the need to grow single crystals.

Acknowledgments. It is a pleasure to thank Professors H. Eisenberg and J. Gillis, Drs. S. Reich and R. Josephs, and Mr. M. Reich for helpful discussions and Drs. Reich and Josephs for their assistance in the optical transform demonstration.

Appendix A

In this appendix, the use of the technique of specific site labeling (SSL) is made to indicate how a unique structure of molecules in solution can be calculated from the measured spatial correlations of the scattering fluctuations.

Let us add to the scattering density of the molecule $\rho(r)$ a labeled site at a point r_0, which can be chosen to lie on the z axis. The labeled site means in the generalized sense a localized strong scattering center, of size smaller than the resolution one intends to achieve.

The SSL has the scattering density:

$$\rho^{H}(r) = \rho(r) + b\delta(r - r_0) \tag{A1}$$

The new scattering amplitude is given by:

$$A^{H}(\kappa) = A(\kappa) + (2\pi)^{-3/2} b e^{i\kappa \cdot r_0} \tag{A2}$$

and the scattering intensity is:

$$S^{H}(\kappa) = S(\kappa) + 2Re[(2\pi)^{-3/2} A(\kappa) b^* e^{-i\kappa \cdot r_0}] + \frac{|b|^2}{(2\pi)^3} \tag{A3}$$

The experimentally measured correlations will be assigned as $C^{H}(\kappa_1,\kappa_2)$.

The expansion of $A^{H}(\kappa)$ in spherical harmonics gives:

$$A_{lm}{}^{H}(|\kappa|) = A_{lm}(|\kappa|) + \frac{2}{\pi} i^l b j_l(|\kappa| \cdot |r_0|) \delta_{m0} \tag{A4}$$

Here one uses the fact that r_0 is along the z axis (its polar angle $\Omega_0 = 0$) so that:

$$Y_{lm}(\Omega_0 = 0) = \left(\frac{2l+1}{4\pi}\right)^{1/2} \delta_{l0} \tag{A5}$$

The general idea of using the SSL data for resolving the orientational ambiguities of the different harmonic components is now clear: The newly introduced scattering center at r_0 gives a well-defined contribution to each one of the components of the scattering amplitudes. The choice of r_0 along the z axis is convenient, as it means that except for $m = 0$ all pairs of components A_{lm} and $A_{lm}{}^{H}$ have to be equal. A phase, $e^{im\alpha_l}$, introduced by rotation around the z axis is still a free parameter to be resolved by another SSL. The quantities solved directly from the measured correlations $C(\kappa_1,\kappa_2)$ and $C^{H}(\kappa_1,\kappa_2)$ are S_{lm} and $S_{lm}{}^{H}$. The complex relations between S_{lm} and $A_{lm}{}^{3}$ require hence further mathematical manipulations.

Using the decomposition formula for by-products of spherical harmonics,[3,4] the components of $S^{H}(\kappa)$ are given by:

$$S_{lm}{}^{H}(|\kappa|) = S_{lm}(|\kappa|) + H_{lm}(|\kappa|) + \frac{|b|^2}{(2\pi)^3} \delta_{l0} \delta_{m0} \tag{A6}$$

where:

$$H_{lm}(|\kappa|) = \frac{1}{\pi} \sum_{l_1 l_2} \{b^*(-1)^m (-i)^{l_2} A_{l_1 m} \cdot (|\kappa|) j_{l_2}(|\kappa| \cdot |r_0|)(2l_2 + 1)^{1/2} + b(-1)^{l_2} (+i)^{l_1} A_{l_2 - m}(|\kappa|) j_{l_1}(|\kappa| \cdot |r_0|)(2l_1 + 1)^{1/2}\}$$

$$\cdot \begin{pmatrix} l_1 & l_2 & l \\ m & 0 & -m \end{pmatrix} \begin{pmatrix} l_1 & l_2 & l \\ 0 & 0 & 0 \end{pmatrix} \left[\frac{(2l_1+1)(2l_2+1)(2l+1)}{4\pi}\right]^{1/2}$$

$$\equiv \sum_{l_1} M_{ll_1}{}^m(|\kappa|\cdot|r_0|)A_{l_1m}(|\kappa|) \quad \text{(A7)}$$

If we approximate the structure by its first L spherical components, we obtain for $L < l < 2L$ and $L < |m| < l$:

$$H_{lm}(|\kappa|) = 0 \quad \text{(A8)}$$

The quantities $S_{lm}{}'$ solved via eq 25–27 are related to the "true" S_{lm} of eq 13 by unknown rotations. So do the $S_{lm}{}^{H'}$ which are obtained from the SSL. If we assign $R = \mathbf{R}(\omega_l)$ as the angles of rotation for $S_{lm}{}'$ and $R^H{\cdot}R = \mathbf{R}(\omega_l{}^H)$ for $S_{lm}{}^{H'}$ we can write:

$$[(S^HR^H - S)R]_{lm} = \sum_{l_1} M_{ll_1}{}^m A_{l_1m} \quad (m \le L) \quad \text{(A9)}$$

and

$$(S^HR^H - S)_{lm} = 0 \quad (m > L) \quad \text{(A10)}$$

These relations used for different values of κ can be used to derive $A_{lm}(\kappa)$ as well as ω_l, $\omega_l{}^H$, and $|r_0|$.

References and Notes

(1) Coherent scattering from different particles can usually be decreased in x-ray and neutron scattering at high enough dilutions. This is obviously not the case in scattering of laser light. The application of spatial correlation for this case will be treated separately.
(2) H. B. Stuhrmann, *Acta Crystallogr., Sect. A.*, **26**, 297–306 (1970).
(3) H. B. Stuhrmann, "Neutron Scattering for the Analysis of Biological Structures", Brookhaven Symposia in Biology, 1975, No. 27, p IV-3.
(4) A. Messiah, "Quantum Mechanics", North-Holland Publishing Co., Amsterdam, 1961, see Appendices B and C.
(5) A. Guinier, *Ann. Phys. (N.Y.)*, **12**, 161–237 (1939).
(6) P. M. Mittelbach and G. Porod, *Acta Phys. Austriaca*, **15**, 122–147 (1962).
(7) As $S_{lm} = (-1)^m S_{l-m}{}^*$ one can use a representation for which S_{lm} is real.
(8) In preparation.

Transport Coefficients of Helical Wormlike Chains. 1. Characteristic Helices †

Hiromi Yamakawa,* Takenao Yoshizaki, and Motoharu Fujii

Department of Polymer Chemistry, Kyoto University, Kyoto, Japan.

Received April 11, 1977

ABSTRACT: The translational diffusion coefficient and intrinsic viscosity of the characteristic regular helix corresponding to the minimum configurational energy of the helical wormlike chain are evaluated by an application of the Oseen–Burgers procedure of hydrodynamics to the cylinder model. The model is discussed in relation to the transport length scales to be adopted, and the possible effect of the coupling between translational and rotational motions is examined. Evaluation is carried out with the use of the Oseen hydrodynamic interaction tensor nonpreaveraged or preaveraged. The results may be written in terms of four model parameters: the total contour length L, the diameter d of the cylinder, and the radius ρ and pitch h of the helix. In all cases, the asymptotic solutions are found. In the case of the preaveraged Oseen tensor, the numerical solutions are also obtained.

Recently, we proposed a very general continuous model, called the helical wormlike chain,[1,2] for stiff or flexible chain macromolecules of all types, and already developed the statistical mechanical theory for some of its equilibrium properties.[2–6] In the present series of papers, we study its steady-state transport properties. The model may be regarded as a hybrid of the three extreme forms of rod, random coil, and regular helix. Thus, first in this paper, we evaluate the translational diffusion coefficient, which is related to the sedimentation coefficient, and the intrinsic viscosity of the characteristic regular helix,[1] i.e., one of these extreme forms corresponding to the minimum configurational energy of the model chain.

As in the case of the Kratky–Porod (KP) wormlike chain,[7–9] evaluation is carried out by an application of the Oseen–Burgers procedure of hydrodynamics to cylinder models, the cylinder axis or chain contour being a regular helix for the present case. The procedure is rather well established for the KP wormlike cylinder, but two new fundamental problems to be considered arise for the present model and therefore also for the helical wormlike cylinder. One is in the hydrodynamic molecular model itself and the other in the hydrodynamic analysis of the frictional force. As previously discussed,[1] the shift factor M_L, as defined as the molecular weight per unit contour length of the helical wormlike model, is closely related to the length scales to be adopted for a given real chain which is replaced by the former, and such length scales depend, to some extent, on the latter and also on the property or behavior to be considered. Thus, the values of M_L and also of the radius and pitch of the characteristic helix determined for various real chains from their characteristic ratios and persistence vectors do not necessarily apply to the transport properties. This is the first problem. The second fundamental problem is to examine the effect of the coupling between translational and rotational motions such that cross terms occur in the generalized 6×6 diffusion tensor of skew bodies like the regular helix.[10,11] Note that the coupling of this kind does not occur for nonskew bodies like rigid rods and rings.

Thus, in section I, the hydrodynamic molecular model is discussed in relation to the length scales to be adopted. In section II, a formal solution for the instantaneous frictional force of the helical cylinder is obtained in the Oseen–Burgers approximation without preaveraging the Oseen hydrodynamic interaction tensor. In sections III and IV, the translational diffusion coefficient and intrinsic viscosity are evaluated, respectively, each with the Oseen tensor nonpreaveraged or preaveraged. In particular, a large part of section III is devoted to a rather detailed discussion of the coupling effect. In all cases, the asymptotic solutions are found. For the case of the preaveraged Oseen tensor, the numerical solutions are also obtained.

(I) Hydrodynamic Molecular Model

As stated in our hypothesis on polymer chain configurations,[1] the length scales to be adopted in the replacement of

† This paper is contributed to the celebration of the 80th birthday of Dr. Maurice L. Huggins, in recognition of his lasting contributions to polymer science.